

The Periodic, Electrochemical Codeposition of Cadmium and Tellurium

A mathematical model is presented for the codeposition of cadmium and tellurium onto a rotating-disk electrode. The treatment incorporates the equation of convective diffusion for liquid phase mass transport, Butler-Volmer expressions for charge-transfer reactions, and a thermodynamic model for individual component activities in the solid state. Because of the formation of CdTe, a compound that has a large negative free energy of formation, the cadmium deposition reaction occurs at potentials substantially positive to its standard electrode potential ($U^\theta = -0.40$ V). This reaction, along with the deposition of tellurium ($U^\theta = +0.55$ V), produces an electrodeposits that contains cadmium, tellurium, and cadmium telluride. The model can be used to calculate transient current-potential relationships, ionic concentration profiles, and deposit compositions. Transport and kinetic parameters for cadmium and tellurium deposition are reported; a multidimensional optimization routine is used to evaluate physiochemical parameters from experimental data for the codeposition process.

M. W. Verbrugge and C. W. Tobias

Department of Chemical Engineering
University of California at Berkeley and
Materials and Molecular Research Division
Lawrence Berkeley Laboratory
Berkeley, CA 94720

Introduction

The unique properties of cadmium telluride, CdTe, were recognized as early as 1856 (Tibbals, 1909). As reflected by the voluminous literature devoted to this material, CdTe is probably the most extensively studied wide band gap, II-VI compound (Aven and Prener, 1967). A number of monographs (Zanio, 1978, and references cited therein) are dedicated exclusively to CdTe. Cadmium telluride materials have found applications in gamma-ray and x-ray spectrometers, electrooptic and acousto-optic modulators, liquid-crystal imaging devices, and as solar-cell materials.

One of the most promising applications of CdTe lies in the fabrication of photovoltaic devices. In 1956, Loferski presented a theoretical treatment to aid in the selection of the optimum semiconductor for photovoltaic solar energy conversion. The semiconductor yielding the highest maximum efficiency, defined as the ratio of the maximum electrical power output to the solar power flux incident to the semiconductor surface, was CdTe. In the present work, we report the determination of transport and kinetic parameters relevant to the electrochemical codeposition of Cd and Te, and we provide a mathematical

model representing this codeposition with a periodic cell current.

It has been observed by numerous researchers that the phase structure and morphology of alloy deposits can be altered by changing the characteristics of the cell-current waveform (Puippe and Ibl, 1980). [The nature of alloy deposits has been variously defined. Faust (1940) defined alloy deposition as "... any process where two or more metals are codeposited intentionally and in which, due to this codeposition, special properties are imparted to the electrode." Brenner (1963) adopted the *Metals Handbook* (Lyman, 1948) definition: "A substance that has metallic properties and is composed of two or more chemical elements of which at least one is a metal. Brenner modified this with the following: "For practical purposes, we can consider a metallic substance as an alloy if the individual constituents cannot be seen by the unaided eye." Physical chemists usually adopt a more restrictive definition. Seitz (1943) refers to alloys as being either substitutional or interstitial. In the state of complete order, each phase is said to have developed a superlattice. For some chemical systems, the alloy forms only for a fairly definite composition, and a superstructure always exists. Mott and Jones (1958) state that such alloys are more properly called compounds. This is the case for CdTe.] In work related to the present study, we report the influence of a pulsed current source on the Cd-Te deposit morphology and photovoltaic properties

The present address of M. W. Verbrugge is General Motors Research Laboratories, Warren, MI 48090.

(Verbrugge, 1985). Although pulsing the cell current provides a useful means for improving deposit quality, this mode of operation requires a more sophisticated mathematical analysis, relative to steady state processes, to predict deposit composition.

Thin films of CdTe have been prepared by chemical vapor deposition, vacuum evaporation, and electrodeposition processes. As is the case in the present study, most CdTe electrodeposition processes make use of an aqueous cadmium sulfate, tellurium dioxide, sulfuric acid electrolyte (Danaher and Lyons, 1978; Panicker *et al.*, 1978; Fulop *et al.*, 1982; Engelken, 1983; Gerritsen, 1984; Takahashi *et al.*, 1984; Uosaki *et al.*, 1984; Lyons *et al.*, 1984; Bhattacharya, 1984). Thin-film electrodeposits have also been formed from nonaqueous solvents (Darkowski and Cocivera, 1985), and from aqueous potassium cyanide electrolytes (Skylas-Kazacos, 1983). Since the costs associated with thin-film electrodeposition processes are generally less than those with other thin-film fabrication techniques, the present study should be relevant to the fabrication of large-area CdTe solar cells.

Because of the low solubility of TeO_2 in aqueous solutions—the maximum concentration of HTeO_2^+ is ≈ 0.001 M (Issa and Awad, 1954)—the Cd^{2+} ion concentration may also be chosen to be sufficiently low (≈ 0.1 M) so that dilute-solution transport theory (Newman, 1973) can be applied. There is a large free energy associated with the formation of CdTe, and hence the composition-dependent thermodynamic properties of the solid state must be taken into account in modeling the electrodeposition process. To account for deviations from ideal behavior, a thermodynamic model is incorporated into the alloy deposition analysis to describe the activity of the individual components in the electrodeposit. Engelken and Van Doren (1985) have incorporated the same thermodynamic model for the solid state in their analyses for the steady state electrodeposition of II-IV and III-V compounds. White *et al.* (1977) have modeled a codeposition system incorporating a homogeneous electrochemical reaction. Pesco and Cheh (1985) have treated steady state alloy electrodeposition processes for systems with a nonuniform current distribution. Beauchamp (1985) has developed a one-dimensional model for the pulsed electrodeposition of alloys. Menon and Landau (1985) have modeled cells with nonuniform current distribution and included unsteady-state effects. Except for the work of Engelken and Van Doren, these models do not take into

account nonideal behavior in the solid state. The models are useful, however, for the treatment of chemical systems that form a deposit wherein the activity of each constituent is equal to its mole fraction. White *et al.* studied the electrodeposition of Cu with very small amounts of Fe codeposited. Pesco and Cheh, Beauchamp, and Menon and Landau compared their model results to experimental data obtained from the codeposition of Pb and Sn.

The schematic diagram of the electrodeposit-electrolyte interface in Figure 1 can help clarify the salient features of our model work. For a dilute liquid phase, ion-ion interactions are negligible and the dilute-solution equation of convective diffusion can be applied to evaluate $c_i(t, y)$, the concentration of reactant or product species in the neutral liquid phase. For solutions of high ionic strength and dilute in reacting ions, the diffuse portion of the double layer will not change significantly in structure, and the potential drop across this region of charge separation can be neglected for highly conductive, well-supported solutions. The inner edge of the diffuse portion of the double layer is the outer Helmholtz plane (OHP), which represents the plane of closest approach for the nonspecifically adsorbed ions. Immediately adjacent to the electrode surface is the inner Helmholtz plane (IHP), where solution species can be specifically adsorbed to the electrode surface. Since specific adsorption is dependent on electrodeposit-solution interactions, and since it is not included in our model, the rate constants measured for Cd and Te electrodeposition may have to be altered in an attempt to match experimental and calculated results, as the CdTe surface may specifically adsorb species differently from the Cd or Te surfaces. In general, the IHP poses a very difficult region to quantify. In this study, the last region of interest, the forming electrodeposit, is assumed to contain three species in equilibrium: Cd, Te, and CdTe (Panicker *et al.*, 1978). Due to the low bulk concentration of HTeO_2^+ , the deposit growth rate is slow and does not significantly influence the fluid dynamics.

The most accessible experimental variables are the total cell current and the potential of the working electrode with respect to a suitable reference. For this reason, we shall compare calculated polarization curves with those obtained by experiment. It is also possible to compare the predicted and measured electrodeposit composition, but this is a more difficult task and would probably provide less insight. Too little electrodeposit is formed to allow accurate determination of the composition by deposit dissolution and subsequent quantitative analysis. (Only thin-film deposits were formed because thick deposits tend to acquire a roughened surface and affect the fluid flow, thus impairing the chances for successful comparison of experiment with theory.) There are a number of other *ex situ* analysis techniques, although they do not appear as quantitative or convenient as theoretical-experimental comparisons of polarization curves obtained in alloy electrodeposition processes. Swathirajan (1986) presents support for the use of *in situ* acquisition of cell current-potential characteristics, and subsequent comparison with theoretical calculations, in order to investigate electrochemical stripping experiments of alloy electrodeposits, in lieu of *ex situ* surface analysis techniques.

Physicochemical Parameters for Cd and Te Electrodeposition

In the following sections we discuss the electrodeposition of Te and Cd. The measured physicochemical parameters for Te

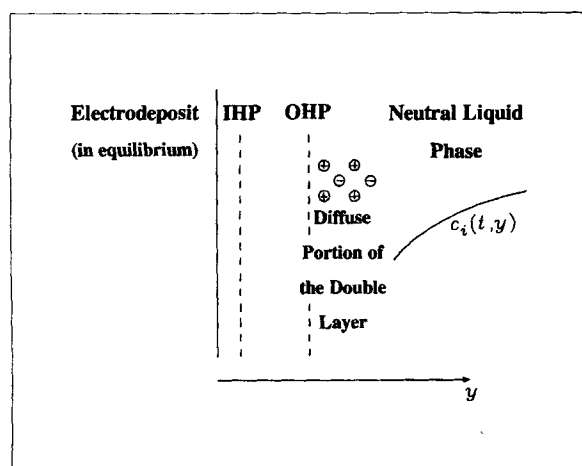


Figure 1. Electrodeposit, interface, and liquid phase.
IHP, Helmholtz plane; OHP, outer Helmholtz plane

electrodeposition and Cd electrodeposition are then used to mathematically model the codeposition of Te and Cd onto a rotating-disk electrode (RDE). The reactions relevant to the study are listed in Table 1. In all these deposition studies, 0.3 M H₂SO₄ was used as supporting electrolyte. The Cd²⁺ species was obtained by adding cadmium sulfate, and the HTeO₂⁺ species resulted from adding tellurium dioxide to the electrolyte (reaction 6 of Table 1). Both glassy carbon and polycrystalline cadmium disk electrodes were used. Standard metallographic polishing techniques were used to remove all projections greater than one micron in height. The electrodes were cleaned with a dilute nitric acid solution before each experiment. The potential of the working electrode was measured against a mercury-mercurous sulfate reference electrode. A Princeton Applied Research model 173 potentiostat/galvanostat controlled the operation of the cell; an Interstate F77 function generator was used with the potentiostat/galvanostat. The data were stored on a Nicolet 1090A digital oscilloscope and later transferred to an HP9825A computer.

The aqueous sulfuric acid electrolytes were prepared from analytical reagent grade chemicals and distilled water that was passed through a Culligan water purification unit consisting of an organic trap, a deionizer, and a microfilter. The specific resistance of the treated water was 15 MΩ · cm. Nitrogen, first equilibrated with a similar electrolyte, was bubbled through the cell solution for 1 h prior to the experiments. A nitrogen atmosphere was maintained above the electrolyte during the experiments.

The primary factor limiting the rate of CdTe electrodeposition is the mass-transfer resistance of the discharging HTeO₂⁺ ion. This is due to low solubility of TeO₂ in aqueous sulfuric acid solutions. Since there is very little HTeO₂⁺ in solution relative to the concentration of Cd²⁺, the HTeO₂⁺ species quickly becomes diffusion-limited if a 1:1 mole ratio of Cd to Te is desired in the electrodeposit. If a direct current source is used to form the CdTe electrodeposit, approximately 1:1 CdTe can be produced if the cell-current density is (3/2) × *i*_{lim,HTeO₂⁺}, where *i*_{lim,HTeO₂⁺} is the steady-state, diffusion-limited current density of the HTeO₂⁺ species,

$$i_{\text{lim,HTeO}_2^+} = - \frac{D_{\text{HTeO}_2^+} c_{\text{HTeO}_2^+}^b}{4F \delta_{\text{HTeO}_2^+}} \quad (1)$$

The Nernst diffusion layer thickness (Levich, 1962) for the HTeO₂⁺ species is

$$\delta_{\text{HTeO}_2^+} = 1.612 \left(\frac{D_{\text{HTeO}_2^+}}{\nu} \right)^{1/3} \left(\frac{\nu}{\omega} \right)^{1/2} \quad (2)$$

The factor of 3/2 preceding *i*_{lim,HTeO₂⁺} is required since four moles of electrons are reacted per mole of Te deposited by reaction 2, Table 1, and two moles of electrons are reacted per mole of Cd deposited by reaction 4. (Note that Faraday's law can be used to state *i*_l = *n*_l*F**N*_{*i,l*}/*S*_{*i,l*}. For 1:1 CdTe, *N*_{HTeO₂⁺} = *N*_{Cd²⁺}.)

The tellurium solution chemistry is complex, and Eq. 2 of Table 1 is only an approximation for the HTeO₂⁺/Te electrode processes. Electroanalytical studies of tellurium in the +4 state are presented in the fundamental work of Lingane and Niedrach (1948, 1949). The chemistry of TeO₂ in sulfuric acid solutions is addressed in the work of Flowers *et al.* (1959). The solubility of TeO₂, which limits the rate of CdTe electrodeposition in aque-

Table 1. Reactions

Reaction No.	St. Electrode Potential V	Electrochemical Reaction
Interfacial Reactions		
1*	0.64	Hg ₂ SO ₄ + 2e ⁻ = 2Hg + SO ₄ ²⁻
2	0.55	HTeO ₂ ⁺ + 3H ⁺ + 4e ⁻ = Te + 2H ₂ O
3	0.00	H ⁺ + e ⁻ = 1/2H ₂
4	-0.40	Cd ²⁺ + 2e ⁻ = Cd
5	-0.92	Te + 2e ⁻ = Te ²⁻
Homogeneous Reactions		
6	—	TeO ₂ + H ⁺ = HTeO ₂ ⁺
7	—	Cd + Te = CdTe

*Reaction 1 represents the reference electrode reaction used in the experimental portion of this work.

ous sulfuric acid solutions, was investigated by Schuhmann (1925), who postulated the species in solution to be HTeO₂⁺ and electrode reaction 2 of Table 1. Issa and Awad (1954) studied the solubility of TeO₂ in aqueous HCl and buffered solutions. Cheng (1961) noted that the sulfate electrolytes yielded a slightly higher solubility than a number of other inorganic salts he studied. Dutton and Cooper (1966) have reviewed analytical work on the oxides and oxyacids of tellurium, and later Cooper (1971) published a treatise on the element Te and its unique chemistry.

In the present work, the diffusion coefficient of the HTeO₂⁺ species, *D*_{HTeO₂⁺}, was calculated from limiting-current experi-

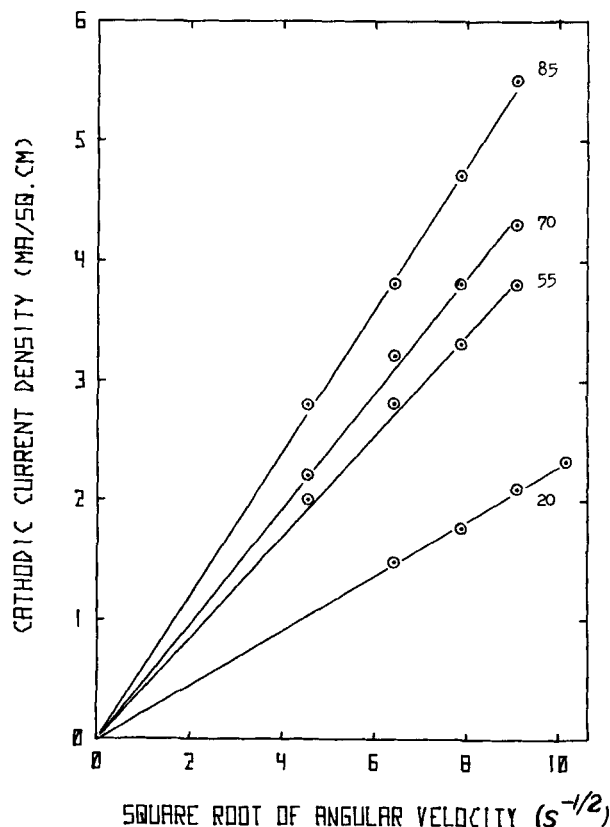


Figure 2. Levich plots for HTeO₂⁺ at various temperatures.

System temperature in °C is listed as a parameter; diffusion coefficients are listed in Table 2.

ments. The 0.001 M HTeO_2^+ /0.3 M H_2SO_4 aqueous electrolyte was maintained at 20°C; the calculated diffusion coefficient is $9.4 \times 10^{-6} \text{ cm}^2/\text{s}$. The resulting Levich plot is shown in Figure 2 for the 20°C experiment, as well as for similar experiments conducted at 55, 70, and 85°C.

Knowledge of the temperature dependence of $D_{\text{HTeO}_2^+}$ is of value since CdTe is often electrodeposited at higher temperatures to obtain large grain deposits with superior electronic properties. At these higher temperatures, the solubility of TeO_2 is still low relative to CdSO_4 (the soluble salt used to place Cd^{2+} in solution), and a direct-current-density source equal to $(3/2) \times i_{\text{lim,HTeO}_2^+}$ can still be used to deposit approximately 1:1 CdTe. In order to obtain 1:1 CdTe and use the $(3/2) \times i_{\text{lim,HTeO}_2^+}$ estimate for the cell-current density, $D_{\text{HTeO}_2^+}(T)$ must be known for all temperatures, as can be seen from Eq. 1. The approximate relationship

$$\frac{D_i \mu}{T} \approx \text{constant} \quad (3)$$

is frequently employed (Bird *et al.*, 1960), where μ is the solution viscosity. For the aqueous H_2SO_4 - HTeO_2^+ solutions analyzed in this work, the average value of the constant in Eq. 3 was $3.04 \times 10^{-10} \text{ cm} \cdot \text{g/s}^2 \cdot \text{K}$ with a standard deviation, weighted over the four temperatures, of $0.014 \times 10^{-10} \text{ cm} \cdot \text{g/s}^2 \cdot \text{K}$. Table 2 lists the temperature dependence of the solution transport properties. Handbook values were used for the electrolyte viscosity.

Triangular current-sweep chronopotentiometric experiments were conducted on this system to obtain the kinetic parameters of reaction 2 in Table 1. The technique developed by the authors was used to construct the theoretical response to the triangular current sweep (Verbrugge and Tobias, 1985a). A symmetry factor of 0.1 and an exchange-current density of 2.0 mA/cm², based on bulk ionic concentrations and unit activity of the electrodeposit, were found to best represent the experimental data.

The electrode potential at which the Cd deposition reaction occurs, reaction 4 of Table 1, can be used to approximate the potential at which 1:1 CdTe can be deposited from an aqueous sulfuric acid electrolyte. Because of the low solubility of TeO_2 , the mass transfer of the HTeO_2^+ species usually limits the rate of Te deposition. No matter how much more cathodic the electrode potential is driven, the rate of Te deposition remains nearly constant ($c_{\text{HTeO}_2^+}^{\text{surf}} \approx 0$), and the added cathodic potential is used only to increase the rate of Cd deposition. For this reason, knowledge of the electrode-kinetic behavior of reaction 4 is an important aspect in the understanding of CdTe electrodeposition processes.

Table 2. Transport Properties of Te Deposition Electrolyte

Temp. K	Viscosity g/cm-s	Diffusion Coeff. cm ² /s	$\frac{D_{\text{HTeO}_2^+} \mu}{T}$ cm-g/K-s
293	0.010	9.4×10^{-6}	3.21×10^{-10}
328	0.0050	2.0×10^{-5}	3.05×10^{-10}
343	0.0041	2.4×10^{-5}	2.87×10^{-10}
358	0.0034	3.2×10^{-5}	3.04×10^{-10}

Limiting-current experiments, analogous to those described in the Te deposition section, were conducted to obtain $D_{\text{Cd}^{2+}}$. The 0.10 M CdSO_4 /0.3 M H_2SO_4 electrolyte was maintained at 23°C; the calculated value for $D_{\text{Cd}^{2+}}$ is $3.7 \times 10^{-6} \text{ cm}^2/\text{s}$. Since the CdTe electrodeposition process is less affected by the Cd^{2+} transport, relative to the HTeO_2^+ transport, the temperature dependence of $D_{\text{Cd}^{2+}}$ will not be discussed. We report (Verbrugge and Tobias, 1985a) for the diffusion coefficient of the Cd^{2+} species in a 0.0058 M CdSO_4 /0.25 M K_2SO_4 electrolyte $D_{\text{Cd}^{2+}} = 3.6 \times 10^{-6} \text{ cm}^2/\text{s}$. Since $D_{\text{Cd}^{2+}}$ is nearly identical in the two solutions, we have a strong indication that there are no significant ion-ion interactions, only ion-solvent interactions, and that dilute-solution transport equations can be used to analyze these experimental systems. Furthermore, in the aqueous sulfuric acid electrolyte $D_{\text{HTeO}_2^+} = 9.6 \times 10^{-6} \text{ cm}^2/\text{s}$, which is significantly greater than $D_{\text{Cd}^{2+}}$. The HTeO_2^+ complex is rather large, with only one positive charge spread throughout the ion. Consequently, it is probably less solvated and can diffuse faster through solution than the smaller Cd^{2+} species (the concentration gradient of both species being equal), which probably has a larger hydration shell.

In general, the Cd deposition current-potential curve is difficult to duplicate theoretically with a Butler-Volmer electrode-kinetic expression. We (1985a) have investigated the electrodeposition of Cd from an aqueous potassium sulfate electrolyte. A symmetry factor of 0.15 and an exchange-current density of 9.1 mA/cm², based on the bulk concentration of Cd^{2+} and unit deposit activity, were found to best represent the current-potential relationship for the discharge of Cd^{2+} from the sulfuric acid electrolyte.

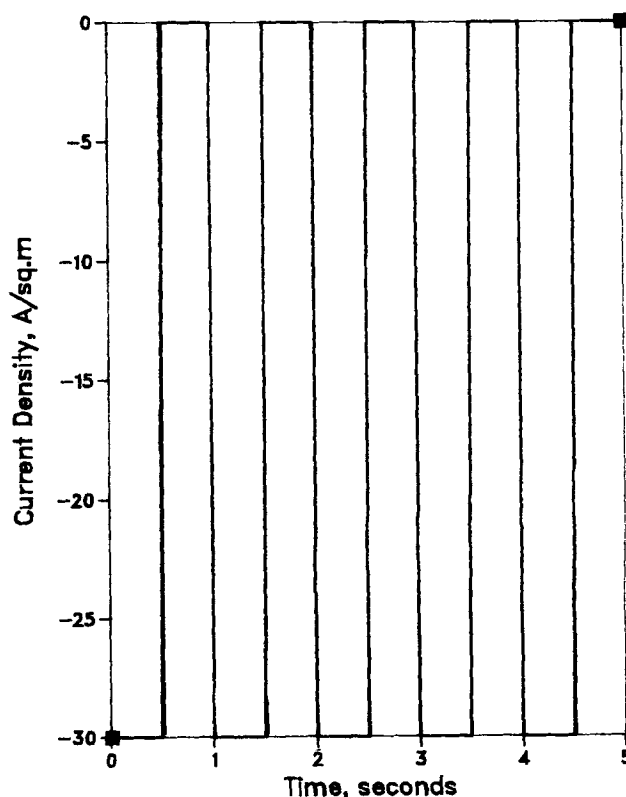


Figure 3. Base case cell-current density.

Table 3. Input Parameters

Quantity	Special or Reaction No.*				Units
	H ₂ TeO ₂ ⁺ 2	H ⁺ 3	Cd ²⁺ 4	Te ²⁻ 5	
c_i^b	1.0×10^{-6}	3.0×10^{-4}	1.0×10^{-4}	0.0	mol/cm ³
D_i	9.4×10^{-6}	9.2×10^{-5}	3.6×10^{-6}	9.3×10^{-5}	cm ² /s
$k_{a,i}$	3.4×10^{-42}	5.0×10^{-12}	7.8×10^5	∞	**
$k_{c,i}$	6.7×10^{-5}	5.0×10^{-12}	1.8×10^{-8}	∞	**
n_i	4	1	2	2	—
r	0	—	—	—	Ω · cm ²
RSAT	1.0×10^{-7}	—	—	—	cm
α	-1.7×10^{-7}	—	—	—	J/mol
β_{act}	6×10^{-5}	—	—	—	—
β_i	0.26	0.50	0.20	—	—
δ_i	0.0058	0.0034	0.0011	0.0034	cm
ρ_o	0.0010	—	—	—	kg/cm ³
$\hat{\rho}_i$	0.049 (Te)	0.077 (Cd)	0.0025 (CdTe)	—	mol/cm ³

*Species entries denoted by subscript i , reaction entries by subscript l on quantities at left.

Optimized results were used for $k_{a,i}$, $k_{c,i}$, α , β_{act} , and β_i .

**The rate-constant units are reaction-dependent. For anodic rate constants, the units are mol/[cm² · s · Π_{*i*}(anodic reactant concentration units) ^{$n_{i,l}$}]. For cathodic rate constants, the exponent $s_{i,l}$ is replaced by $-s_{i,l}$.

Mathematical Analysis for the Periodic Codeposition of Cd and Te

Close to the disk surface, the normal velocity is (Schlichting, 1979)

$$v_y = -0.51023 \omega^{3/2} \nu^{-1/2} y^2. \quad (5)$$

Liquid phase

The one-dimensional equation of convective diffusion is used to describe the mass transport of species i :

$$\frac{\partial c_i}{\partial t} + v_y \frac{\partial c_i}{\partial y} = D_i \frac{\partial^2 c_i}{\partial y^2}. \quad (4)$$

The initial condition and boundary conditions are

$$c_i(0, y) = c_i^b, \quad (6)$$

$$c_i(t, \infty) = c_i^b, \quad (7)$$

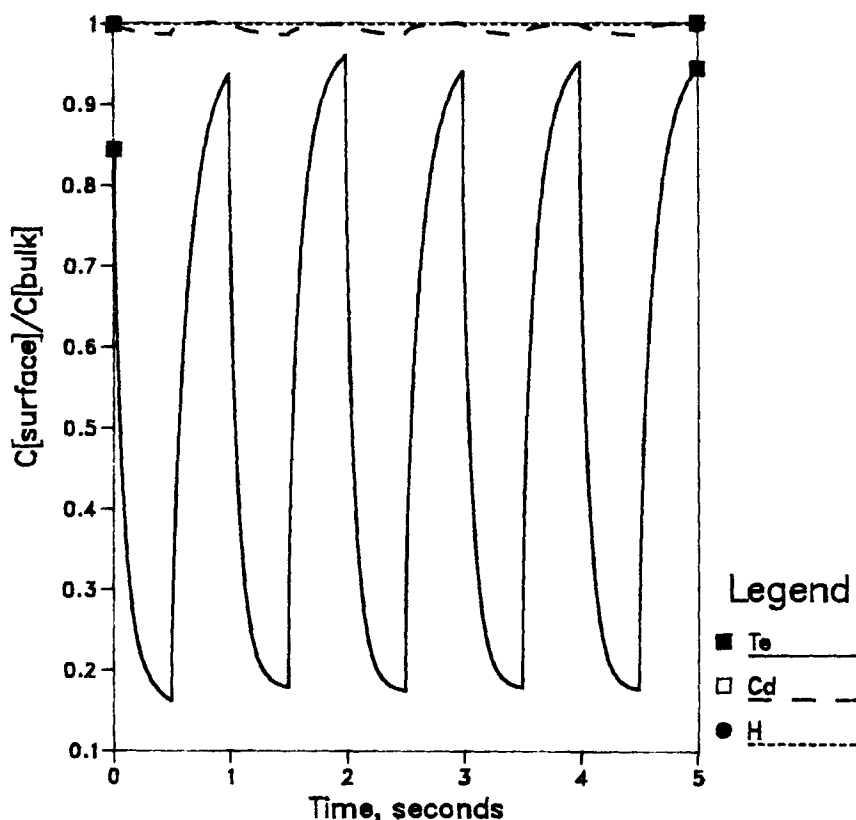


Figure 4. Base case, dimensionless ionic surface concentrations.

and

$$\frac{\partial c_i(t, 0)}{\partial y} = \frac{1}{FD_i} \sum_i \frac{s_{i,l} i_l(t)}{n_i}, \quad (8)$$

where the summation indicates that a species can be involved in more than one electrochemical reaction.

The electrode reaction l can be expressed as

$$n_l e^- \rightleftharpoons \sum_i s_{i,l} M_i^{z_i}. \quad (9)$$

Equation 9 is a general expression for an electrochemical reaction, from which any of the electrochemical reactions listed in Table 1 can be represented.

Equation 4 provides a good representation of the ionic mass transport for systems with large Schmidt numbers, small disk radii, low exchange-current densities, highly conductive electrolytes, and low concentrations of reacting species (Newman, 1966). For the electrodeposition process, subscript i refers to HTeO_2^+ , H^+ , Cd^{2+} , and Te^{2-} , the four ionic species participating in the electrochemical reactions of Table 1. Four convective diffusion equations are written for the four species; the solution to this system of equations yields the surface concentrations of the reactant and product species and the partial current densities of reactions, 2, 3, 4, and 5. It should be noted that the hydro-

gen evolution reaction may have a nonuniform distribution due to the high concentration of H^+ . However, the hydrogen evolution reaction is very slow on the electrodeposited material, and the high kinetic resistance tends to promote a uniform reaction distribution. Usually the codeposition process takes place with high current efficiency, and little hydrogen evolution occurs.

Liquid-electrodeposited interface

A Butler-Volmer electrode-kinetic equation is used to relate the partial current density of the electrochemical reaction l , the surface concentrations of the species participating in the reaction, and the electrode potential. The four electrode-kinetic equations represent reactions, 2, 3, 4, and 5 of Table 1, respectively:

$$\frac{i_2}{4F} = k_{a,2} e^{(1-\beta_2)4fV} a_{\text{Te}} - k_{c,2} e^{-\beta_2 4fV} (c_{\text{HTeO}_2^+}) (c_{\text{H}^+})^3 \quad (10)$$

$$\frac{i_3}{F} = k_{a,3} e^{(1-\beta_3)fV} (p_{\text{H}_2})^{1/2} - k_{c,3} e^{-\beta_3 fV} c_{\text{H}^+} \quad (11)$$

$$\frac{i_4}{2F} = k_{a,4} e^{(1-\beta_4)2fV} a_{\text{Cd}} - k_{c,4} e^{-\beta_4 2fV} c_{\text{Cd}^{2+}} \quad (12)$$

$$\frac{i_5}{2F} = k_{a,5} e^{(1-\beta_5)2fV} c_{\text{Te}^{2-}} - k_{c,5} e^{-\beta_5 2fV} a_{\text{Te}} \quad (13)$$

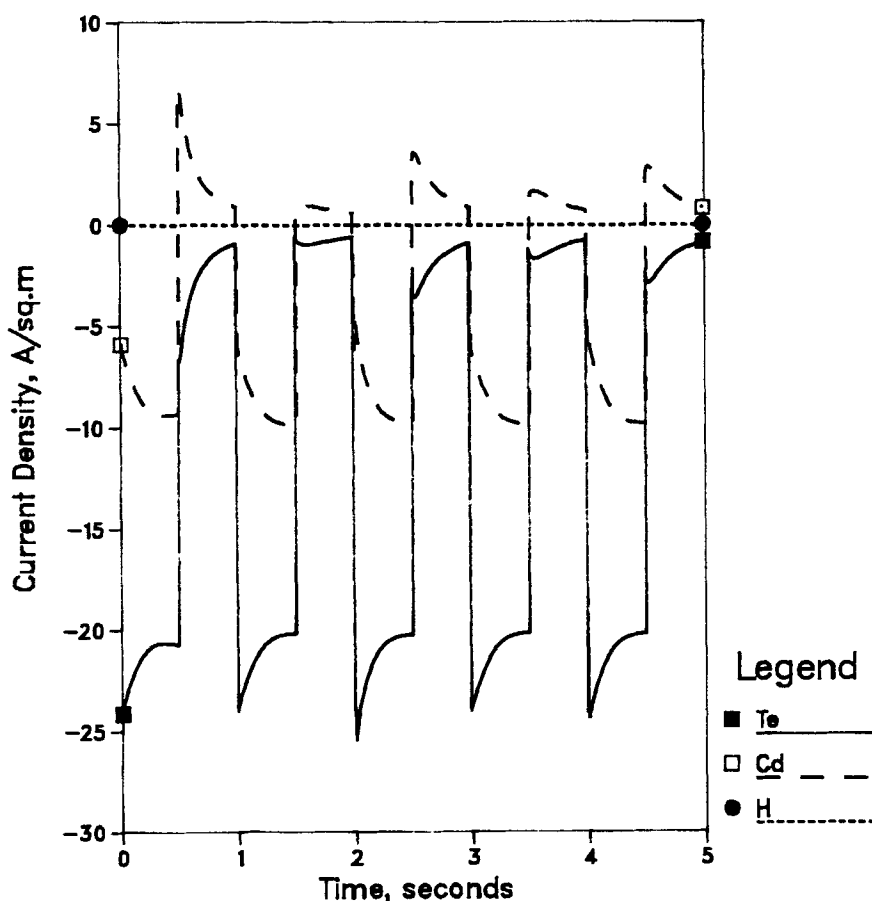


Figure 5. Base case, partial current densities.
Under these conditions, reaction 5 does not take place.

In addition, the sum of the partial current densities must equal the cell-current density,

$$\sum_{l=2}^5 i_l = i_{\text{cell}}. \quad (14)$$

The potential V in Eqs. 10–13 represents the potential difference between the working electrode and a standard hydrogen electrode, corrected for ohmic drop. V is given by

$$V = E + \left[U_{\text{ref}}^0 - \frac{1}{n_{\text{ref}} f} \sum_i s_{i,\text{ref}} \ln c_{i,\text{ref}} \right] - i_{\text{cell}} r, \quad (15)$$

where E is the measured cell potential.

The partial current densities in Eqs. 10–13 couple the convective diffusion equations through the boundary condition given by Eq. 8. The activity of Cd, a_{Cd} , and Te, a_{Te} , is treated in the following section.

Electrodeposit

To evaluate the component activities in the electrodeposit, we shall make use of Jordan's (1970) regular associated solution (RAS) theory. Jordan developed this theory in order to describe mathematically the liquidus curves for the Cd-Te and Zn-Te systems. Since the same three species are present in the solid phase (Cd, Te, and CdTe), we use the same model.

The RAS theory adapted for the Cd-Te-CdTe system contains the assumption that departures from ideal-solution behavior are due to short-range, nearest-neighbor interactions, which are taken into account by identifying the activity coefficients γ_{Cd} , γ_{Te} , and γ_{CdTe} with those of a regular, ternary solution, making use of *interchange energies* for Cd-Te, Cd-CdTe, and Te-CdTe interactions. These expressions can be combined with the Gibbs energy of formation for CdTe (reaction 7, Table 1),

$$\Delta G_{\text{CdTe}} = -RT \ln \frac{a_{\text{CdTe}}}{a_{\text{Cd}} a_{\text{Te}}}. \quad (16)$$

If the interchange energies for Cd-CdTe and Te-CdTe interactions are taken equal, the activities can be approximated as

$$a_{\text{Te}} = \frac{\bar{x}_{\text{Te}} - \bar{x}_{\text{Cd}} + P}{1 + P} \exp \left[\frac{\alpha (\bar{x}_{\text{Cd}})^2}{RT} \right], \quad (17)$$

$$a_{\text{Cd}} = \frac{\bar{x}_{\text{Cd}} - \bar{x}_{\text{Te}} + P}{1 + P} \exp \left[\frac{\alpha (\bar{x}_{\text{Te}})^2}{RT} \right], \quad (18)$$

and

$$a_{\text{CdTe}} = \frac{1 - P}{1 + P} \exp \left[\frac{\alpha}{2RT} (1 - 4\bar{x}_{\text{Te}}\bar{x}_{\text{Cd}}) \right], \quad (19)$$

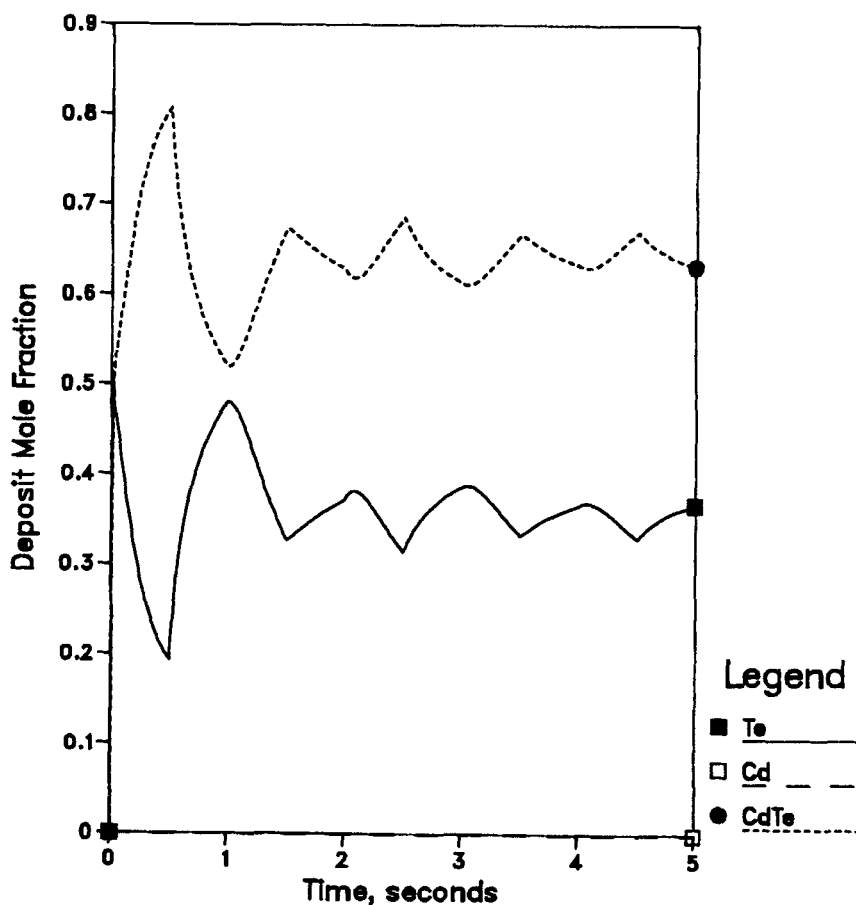


Figure 6. Base case, integrated deposit mole fractions.

where

$$P = [1 - \bar{x}_{\text{Te}}\bar{x}_{\text{Cd}}(1 - \beta_{\text{act}}^2)]^{1/2}. \quad (20)$$

β_{act} is the degree of dissociation at $\bar{x}_{\text{Cd}} = \bar{x}_{\text{Te}} = 0.5$; the overbar has been used to denote atomic mole fractions. Equations 17–20 represent a one-parameter model for the electrodeposit thermodynamics, since the Gibbs free energy of formation for CdTe can be used to eliminate α or β_{act} .

The atomic mole fractions for Te, \bar{x}_{Te} , and Cd, \bar{x}_{Cd} , can be obtained by integrating the appropriate partial current densities:

$$\bar{x}_{\text{Cd}} = \frac{\int_{t_{\text{RSAT}}}^t 2i_4 dt}{\int_{t_{\text{RSAT}}}^t (i_2 + 2i_4 - 2i_5) dt}, \quad (21)$$

and

$$\bar{x}_{\text{Te}} = 1 - \bar{x}_{\text{Cd}}. \quad (22)$$

In these expressions, the time interval from t_{RSAT} to t is required to deposit one relevant surface-activity thickness (RSAT). The RSAT is the depth of deposit that is used to evaluate a surface

composition. This allows us to introduce a length scale into the solid state thermodynamic model. A more complete discussion of the RSAT is provided elsewhere (Verbrugge and Tobias, 1985b).

The *Liquid-electrodeposit Interface* section and the *Electrodeposit* section above provide boundary condition information for the mass transport problem. In these two sections there are ten unknowns: $i_2, i_3, i_4, i_5, V, E, a_{\text{Cd}}, a_{\text{Te}}, x_{\text{Cd}},$ and x_{Te} . These are balanced by the following ten independent equations: 10, 11, 12, 13, 14, 15, 17, 18, 21, and 22. The system of equations is solved by the method of superposition; the numerical method used for these types of problems is presented elsewhere (Verbrugge and Tobias, 1985b). In applying the superposition technique, we used Nisancioglu and Newman's (1974) flux-step solution. A Newton-Raphson routine was employed to iteratively solve the resulting system of equations. This model was combined with an optimization routine (Verbrugge and Tobias, 1985a) to fit the physicochemical parameters to the data. In the next section of this treatment we analyze the periodic electrodeposition process with model and experimental results.

Results of the Proposed Model

The current source used in the theoretical calculations and experimental work is shown in Figure 3. The maximum pulse-current density is $1.23 \times i_{\text{lim, HTeO}_2^+}$. As previously discussed,

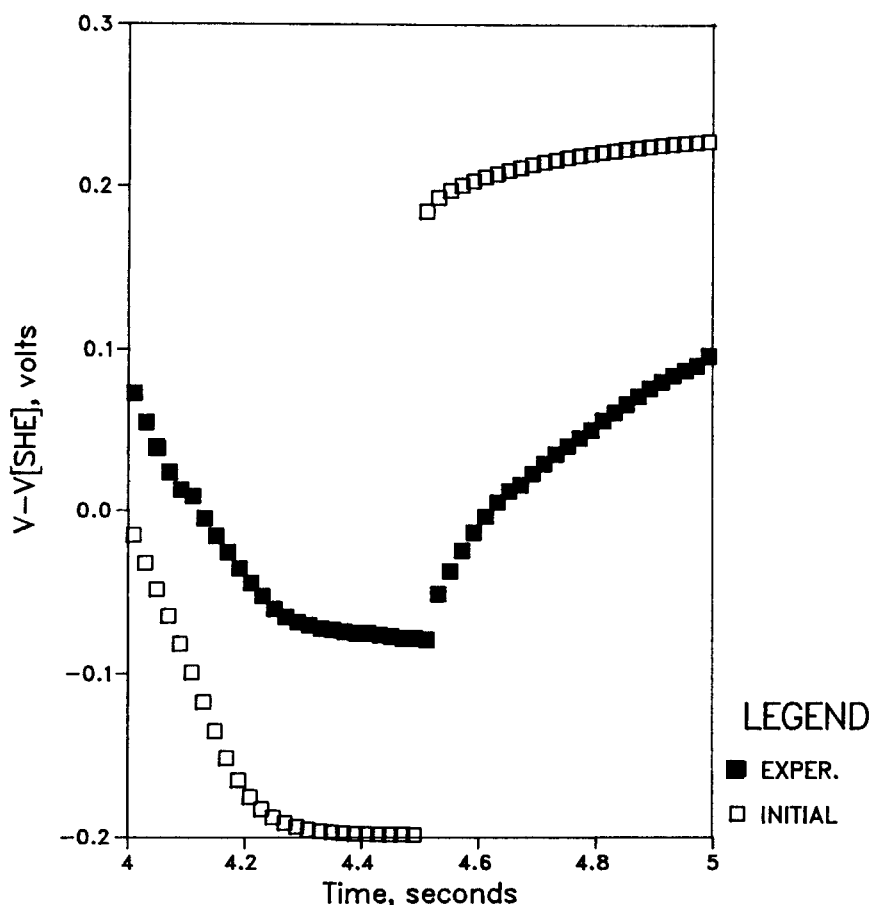


Figure 7. Electrode potential for the deposition process.

No adjustable parameters were used to construct the theoretical curve labeled *Initial*.

$(3/2) \times i_{lim, HTeO_2^+}$ yields nearly 1:1 CdTe. For the 30 A/m² (3 mA/cm²) maximum cathodic current source used in this study, we would expect the Te atomic mole fraction to be greater than 0.5. The input parameters to the computer program are listed in Table 3. In the following discussion we analyze the base case behavior and explain how the input kinetic constants and β_{act} were chosen. In Figure 4 a plot of the ionic surface concentrations is shown. A surface concentration plot is not shown for Te^{2-} since the current due to reaction 5 of Table 1 was insignificant under these conditions, although the rate constants for this reaction were set to high values. Te^{2-} did not form for two reasons. First, Te is attracted to Cd and CdTe in the deposit, thus Te has a suppressed deposit activity and the cathodic term in Eq. 13 is strongly reduced. Second, the electrode potential required to deposit CdTe is significantly more anodic than the -0.92 V standard electrode potential of reaction 5. It should be noted that reaction 5 cannot be dropped from the analysis *a priori*. It is commonly observed in the electrodeposition of pure Te (unit activity in the deposit) that Te^{2-} is formed prior to hydrogen evolution (Lingane and Niedrach, 1948; Jamieson and Perone, 1969; Shinagawa *et al.*, 1977; Barbier *et al.*, 1978). In addition, more cathodic potentials result if larger cathodic currents are used; larger cathodic currents could be used to create a deposit with higher Cd content. As can be seen in Table 3, the bulk concentration of $HTeO_2^+$ is much lower than that of Cd^{2+} . The $HTeO_2^+$ concentration reaches a minimum near the end of the first on-time, when $c_{HTeO_2^+}^{surf}/c_{HTeO_2^+}^b = 0.16$ and $t = 0.5$ s. During

the following off-time, diffusion and convection supply the electrode surface with $HTeO_2^+$ ions from the bulk electrolyte, and the concentration of $HTeO_2^+$ increases until the beginning of the next on-time. This process is repeated over the subsequent cycles. The Cd^{2+} and H^+ species incur little mass transport resistance, and their surface concentrations do not differ significantly from their bulk concentrations under these conditions.

The partial current densities for reactions 2, 3, and 4 are given in Figure 5. At the beginning of the on-time (0 s for the first cycle), reaction 2 supplies most of the current, and the $HTeO_2^+$ surface concentration is reduced. As the $HTeO_2^+$ ion becomes mass-transfer limited, reaction 4 increases in rate and more Cd deposits. During the off-time, Cd dissolves and Te continues to electrodeposit. For these conditions, there is very little hydrogen evolution. Both experimental and theoretical results indicate that the electrodeposition process takes about five cycles to reach a uniform and sustained periodic state. About 1.5 *RSAT* are deposited per cycle. It is the electrodeposit's influence that prolongs the approach to steady state; the surface-concentration profiles reach a periodic state prior to the fifth cycle, as seen in Figure 4. The partial current densities during a particular cycle are dependent on the *RSAT* concentration formed during the previous cycle. It is because of this dependence on the previous cycle that the system oscillates about the uniform periodic state until the fifth cycle.

In Figure 6 the electrodeposit mole fractions are presented for the base conditions. The mole fractions are related to the atomic

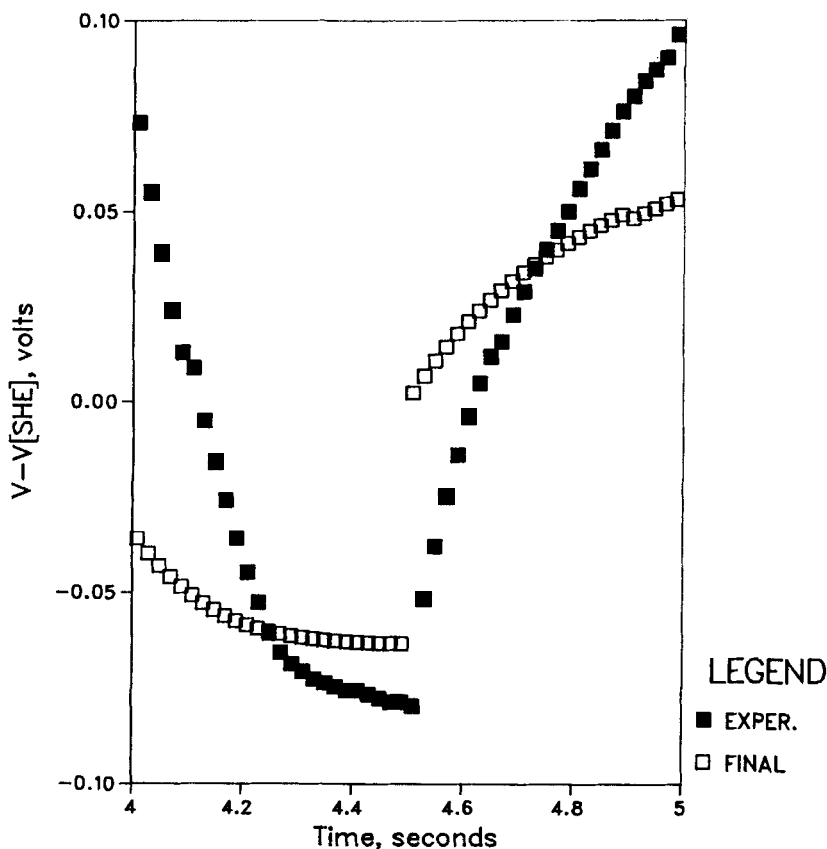


Figure 8. Electrode potential for the deposition process.

The ordinate is different from Figure 7. An optimization routine was used to fit k_{cd} , β_i , β_{act} .

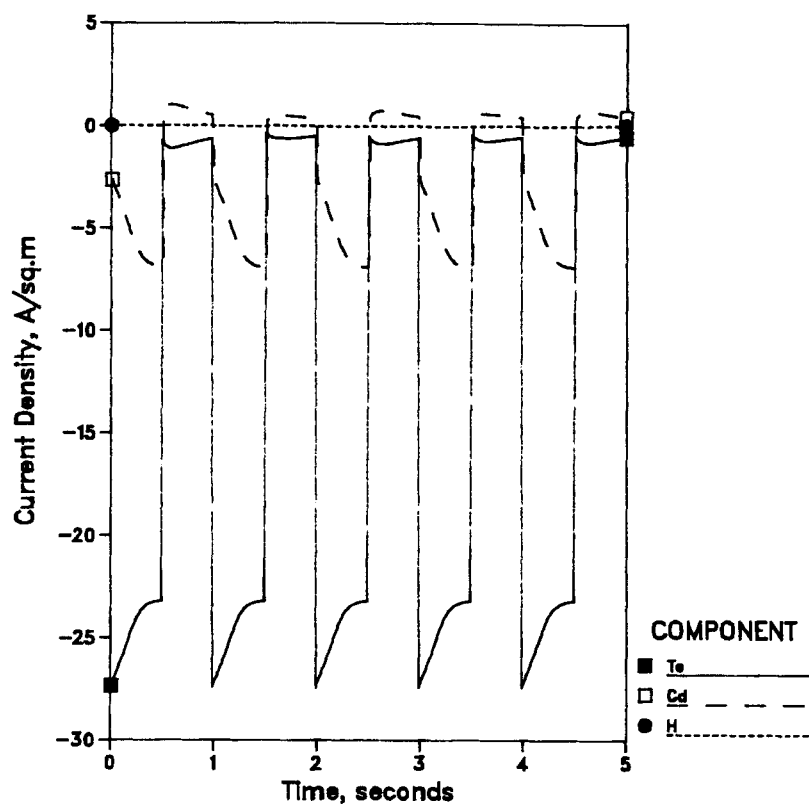


Figure 9. Parametric analysis.

Tellurium deposition rate constants $k_{a,2}$ and $k_{c,2}$ are increased by an order of magnitude relative to base conditions.

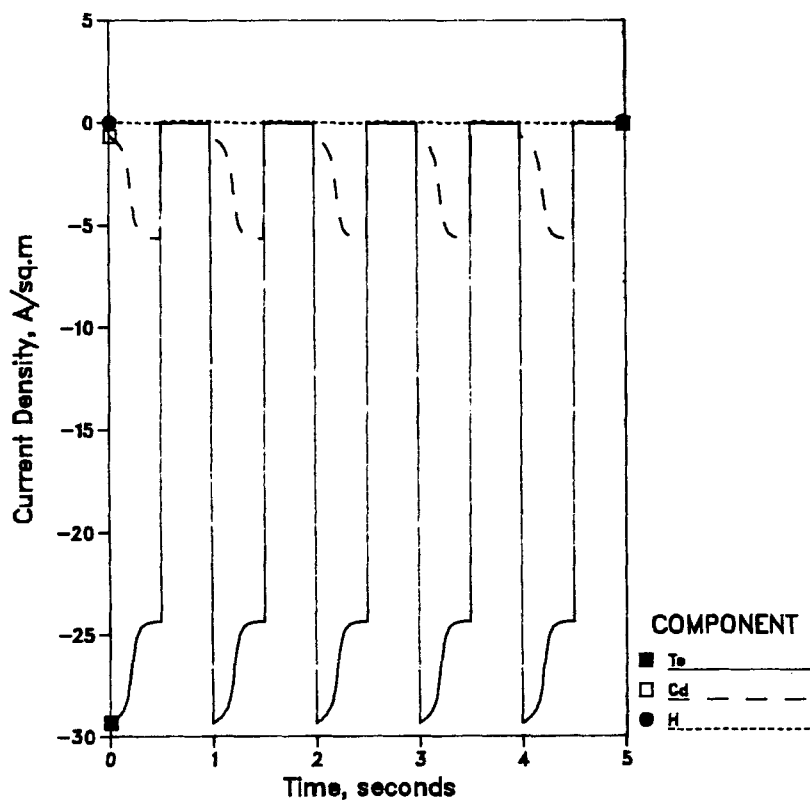


Figure 10. Parametric analysis.

Cadmium deposition rate constants $k_{a,4}$ and $k_{c,4}$ decreased by an order of magnitude relative to base conditions.

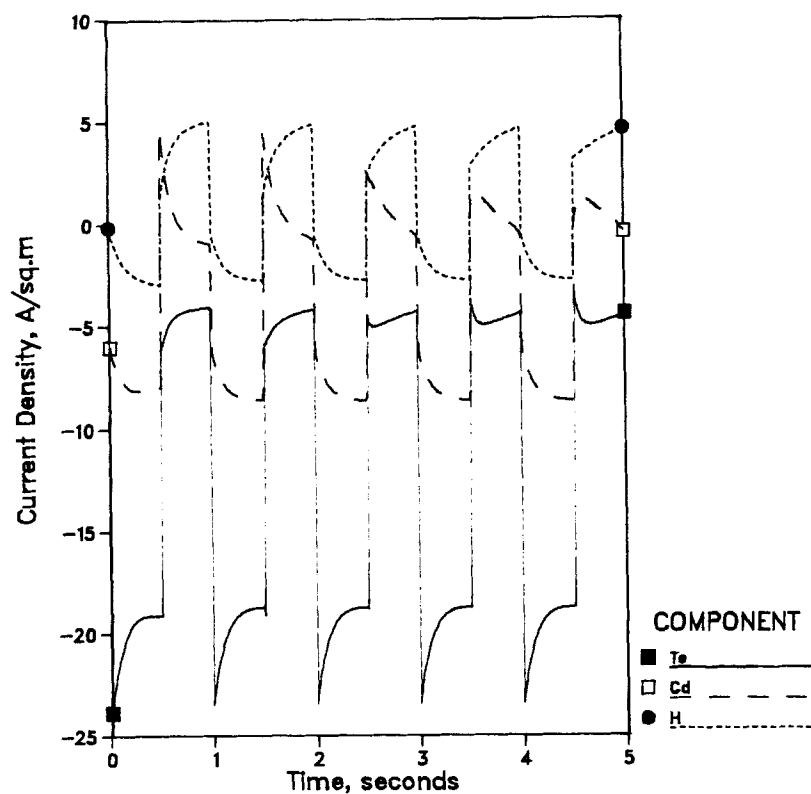


Figure 11. Parametric analysis.

Hydrogen-evolution rate constants $k_{a,3}$ and $k_{c,3}$ increased by an order of magnitude relative to base conditions.

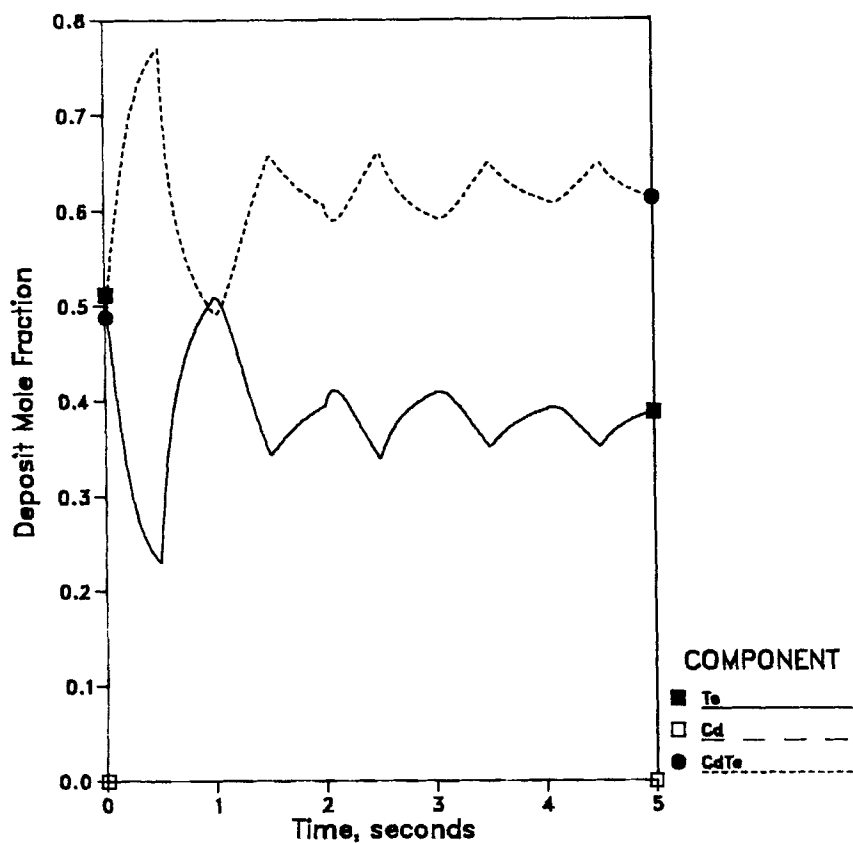


Figure 12. Parametric analysis.

Solid-state dissociation factor β_{ad} increased by an order of magnitude relative to base conditions.

mole fractions by the following equations:

$$x_{\text{Te}} = \frac{\bar{x}_{\text{Te}} - \bar{x}_{\text{Cd}} + P}{1 + P}, \quad (23)$$

$$x_{\text{Cd}} = \frac{\bar{x}_{\text{Cd}} - \bar{x}_{\text{Te}} + P}{1 + P}, \quad (24)$$

and

$$x_{\text{CdTe}} = \frac{1 - P}{1 + P}. \quad (25)$$

As expected, due to the Gibbs free energy of formation of CdTe being large and negative, very little free Cd exists for $\bar{x}_{\text{Cd}} < 0.5$; most of the Cd is present in the CdTe. It can also be seen that during the off-times Cd dissolves and free Te is released into the electrodeposit, which increases the Te mole fraction x_{Te} .

The experimental and calculated electrode-potential behavior is presented in Figures 7 and 8 for the fifth cycle, after the system has reached a periodic state. To construct the theoretical curve in Figure 7 (labeled *Initial*), the measured rate parameters ($k_{a,1}$, $k_{c,1}$, and β_{act}) for Te deposition and Cd deposition were used. In an attempt to force reaction 5 to take place with the current source specified in Figure 3, $D_{\text{Te}^{2-}}$ was set to a high value, as were the rate constants for reaction 5; the ratio of the rate constants is fixed by the standard electrode potential. To better represent the experimental curve, a multidimensional optimiza-

tion routine was used to minimize the difference between the calculated and experimental potential response, the results of which are presented in Figure 8. The optimization routine was not sensitive to the kinetic parameters for H_2 evolution or Te dissolution to produce Te^{2-} . β_{act} was set equal to 0.055 to construct the *Initial* curve in Figure 7, as this was the value Jordan used in his high-temperature experiments. The optimization routine changed this parameter more than any other. The final values of the optimized parameters are listed in Table 3. The shape of the *Initial* curve in Figure 7 resembles the experimental curve. After the optimization routine operates on the model, the resultant *Final* curve in Figure 8 is displaced closer to the experimental curve. It should be noted that the ordinate is different in Figures 7 and 8. The proposed fit solution in Figure 8 does not represent an entirely satisfactory result, although the theoretical solution does remain in a potential region near the experimental curve. To elucidate the behavior of the model, a sensitivity analysis of the optimized parameters is addressed in the following discussion.

The effect of changing the Te deposition rate constants is depicted in Figure 9. If the rate constants $k_{a,2}$ and $k_{c,2}$ are set larger by an order of magnitude, or if a larger symmetry factor is used, more Te is incorporated into the electrodeposit. The periodic state is reached sooner since Cd dissolution from the lower Cd-content deposit is suppressed during the off-time. A uniform and sustained periodic state is reached by the third cycle.

If the Cd kinetic constants are reduced by an order of magnitude, the system reaches a steady state after about two cycles, as

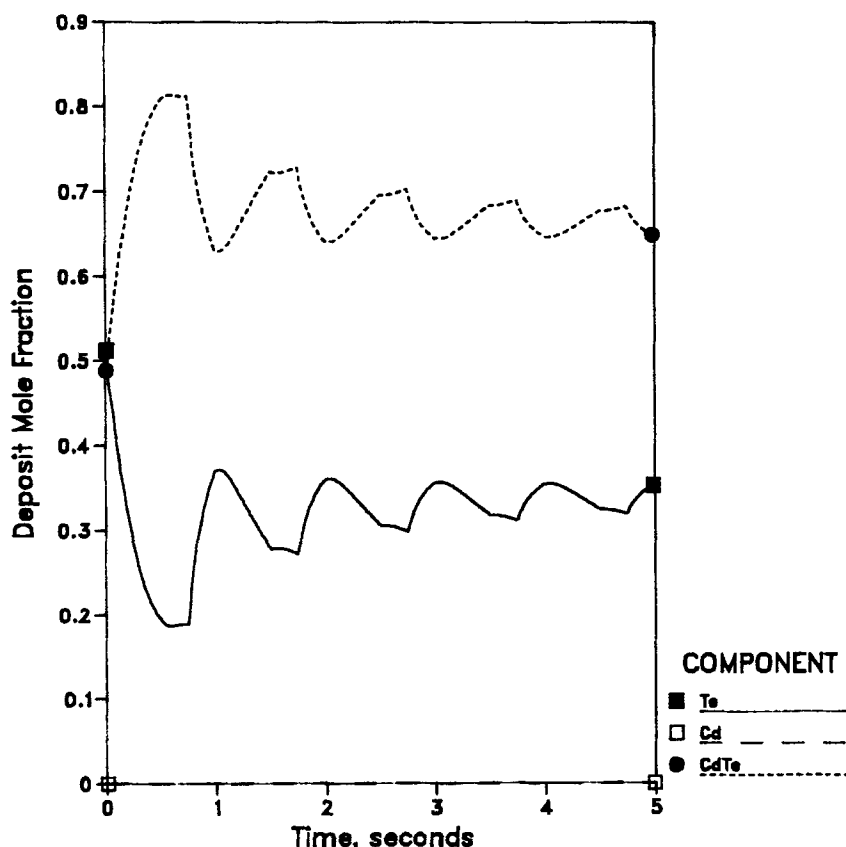


Figure 13. Parametric analysis.

On-time to off-time ratio for cell-current density set to 3:1.

seen in Figure 10. Because the system is more sensitive to the Cd electrodeposition kinetics, a steady state is reached more quickly in Figure 10 than in Figure 9. The system is less sensitive to Te electrodeposition kinetics, reaction 2, because the major obstacle to Te deposition is the HTeO_2^+ mass transfer resistance.

If the hydrogen rate constants are increased by four orders of magnitude, the partial current densities during the deposition process are represented by Figure 11. For this case, H_2 is evolved during the on-time, slightly reducing the Te and Cd deposition rates relative to the base case deposition rates. During the off-time, dissolved H_2 present at low concentration is oxidized to H^+ , and at the end of the off-time both Cd and Te electrodeposit, in contrast to any of the previous cases.

If β_{act} is increased by an order of magnitude, increasing the dissociation of CdTe, the electrodeposit composition history in Figure 12 results. Comparing Figure 12 to the base case deposit, mole fraction plot in Figure 6, we can see that a higher concentration of free Te results with the increased CdTe dissociation.

The mole fraction plot in Figure 13 shows that the CdTe content in the electrodeposit can be increased by specifying an on-time to off-time ratio of 3:1 for the cell-current source, instead of the 1:1 ratio used in the base conditions. Since the HTeO_2^+ species is mass-transfer limited during the majority of the on-time, the Cd^{2+} rate of reaction increases throughout the on-time, as shown, for example, in Figure 5. During the extra on-time in the 3:1 mode of operation more Cd deposits, which combines with Te in the electrodeposit to form CdTe. More cathodic potentials result in the 3:1 mode of operation, and some hydro-

gen evolution occurs during the last part of the on-time. The CdTe content in the electrodeposit can also be increased by increasing the maximum cell current during the on-time. The partial current densities for a maximum cathodic current density equal to twice that of the base conditions are shown in Figure 14. In this mode of operation the HTeO_2^+ species quickly becomes mass-transfer limited, and the rate of Cd deposition increases during the on-time. With the added amount of Cd in the electrodeposit, a larger Cd corrosion current is observed during the off-time. It can also be seen that H_2 begins to evolve during the on-time. The system reaches a uniform and sustained periodic state after the second cycle since about 3 *RSAT* are deposited during the on-time, and the system is nearly driven to a steady state by the end of each on-time.

Conclusions

Due to the increasing demand for thin-film alloys with precisely controlled composition and structure, researchers are beginning to address the quantitative modeling of codeposition processes. In this study we have coupled a thermodynamic description of the electrodeposit with transient convective diffusion equations for the electrolyte species; Butler-Volmer equations written for each charge-transfer reaction relate the equations describing the electrolyte and solid phases. The model shows reasonable agreement with results obtained from the periodic coelectrodeposition of Cd and Te onto a rotating-disk electrode. A more sophisticated model would incorporate dou-

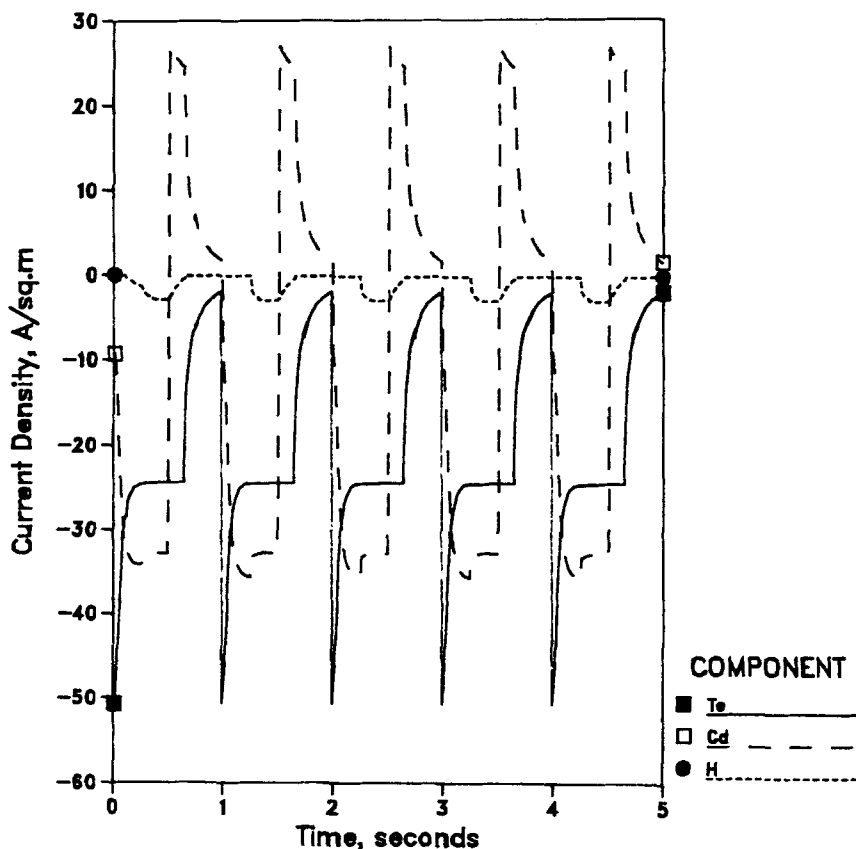


Figure 14. Parametric analysis.

Maximum, cathodic pulse-current density twice that of base condition.

ble-layer adsorption, the capacitance of the double layer (for processes in which the pulsed-current frequency is comparable to, or larger than, the inverse of the characteristic time for the double-layer charging processes), and a more general treatment of the electrodeposit, including solid state kinetic processes.

Acknowledgment

This work was supported by the Director, Office of Energy Research, Office of Basic Energy Sciences, Materials Sciences Division of the Office of the U.S. Department of Energy, under contract No. DE-AC03-76SF00098.

Notation

a_i = surface activity of component i
 c_i = concentration of species i , mol/cm³
 c_i^b = bulk concentration of species i , mol/cm³
 $c_{i,ref}$ = reference electrode compartment concentration of species i , mol/cm³
 D_i = diffusion coefficient of species i , cm²/s
 e^- = an electron
 E = electrode potential relative to the reference electrode, V
 $f = F/RT$, V⁻¹
 F = Faraday's constant, 96487 (C/equiv.)
 i = cell-current density, mA/cm²
 i_l = partial current density for reaction l , mA/cm²
 $k_{a,l}$ = anodic rate constant of reaction l
 $k_{c,l}$ = cathodic rate constant of reaction l
 M_i = chemical formula of species i
 n_i = number of electrons in reaction l
 $N_{i,l}$ = flux of species i corresponding to reaction l , mol/cm² · s
 p_{H_2} = hydrogen partial pressure, atm
 r = cell ohmic resistance, $\Omega \cdot \text{cm}^2$
 R = universal gas constant, 8.314 (J/mol · K)
 $RSAT$ = relevant surface-activity thickness, cm
 $s_{i,l}$ = stoichiometric coefficient of species i in reaction l
 t = time, s
 T = absolute temperature, K
 U_l^0 = standard electrode potential for reaction l , V
 v_y = normal velocity component to a rotating-disk electrode, cm/s
 x_i = molecular mole fraction of species i
 \bar{x}_i = atomic mole fraction of species i
 y = normal distance from the electrode surface, cm

Greek letters

α = interchange energy, J/mol
 β_{act} = degree of CdTe dissociation at $\bar{x}_{Te} = \bar{x}_{Cd} = 0.5$
 β_l = symmetry factor for reaction l
 δ_l = Levich diffusion layer thickness of species i , cm
 ν = kinematic viscosity, cm²/s
 ρ_o = solvent mass density, kg/cm³
 $\hat{\rho}_i$ = species i molar density, mol/cm³
 ω = disk rotation speed, radian/s

Literature cited

Aven, M., and J. S. Prener, eds., *Physics and Chemistry of II-VI Compounds*, Wiley, New York (1967).
 Barbier, M. J., et al., "Electrochemical Study of Tellurium Oxidoreduction in Aqueous Solutions," *J. Electroanal. Chem.* **94**, 47 (1978).
 Beauchamp, C. R., "A Mathematical Model for the Pulsed Electrodeposition of Alloys," *Electrochem. Soc. Meet.*, Abstract 216, Las Vegas (Oct., 1985).
 Bhattacharya, R. N., and K. Rajeshwar, "Electroless Deposition of CdTe Thin Films," *J. Electrochem. Soc.*, **131**, 939 (1984).
 Bird, R. B., et al., *Transport Phenomena*, Wiley, New York (1960).
 Brenner, A., *Electrodeposition of Alloys, Principles and Practice*, 1, Academic Press, New York (1963).
 Cheng, K. L., "Analysis of Lead Telluride with an Accuracy to Better than 0.1%," *Anal. Chem.*, **33**, 761 (1961).
 Cooper, W. C., *Tellurium*, Van Nostrand Reinhold, New York (1971).

Danaher, W. J., and L. E. Lyons, "Photoelectrochemical Cell with Cadmium Telluride Film," *Nature*, **271**, 139 (1978).
 Darkowski, A., and M. Cocivera, "Electrodeposition of Cadmium Telluride Using Phosphine Telluride," *J. Electrochem. Soc.*, **132**, 2768 (1985).
 Dutton, W. A., and W. C. Cooper, "The Oxides and Oxyacids of Tellurium," *Chem. Revs.*, **66**, 657 (1966).
 Engelken, R. D., "An Analysis of the Electrodeposition Process for Cadmium Telluride Thin Film," Ph.D. Thesis, Univ. of Missouri, Rolla (1983).
 Engelken, R. D., and T. P. Van Doren, "Ionic Electrodeposition of II-VI and III-V Compounds," *J. Electrochem. Soc.*, **132**, 2904, 2910 (1985).
 Faust, C. L., "Electrodeposition of Alloys, 1930 to 1940," *Trans. Electrochem. Soc.*, **78**, 1940, 383.
 Flowers, R. H., et al., "Basic Properties of the Dioxides of Group VI-I," *J. Inorg. Nucl. Chem.*, **9**, 155 (1959).
 Fulop, G., et al., "High-Efficiency Electrodeposited Cadmium Telluride Solar Cells," *Appl. Phys. Lett.*, **40**, 327 (1982).
 Gerritsen, H. J., "Electrochemical Deposition of Photosensitive CdTe and ZnTe on Tellurium," *J. Electrochem. Soc.*, **131**, 136 (1984).
 Issa, I. M., and S. A. Awad, "The Amphoteric Properties of Tellurium Dioxide," *J. Phys. Chem.*, **58**, 948 (1954).
 Jamieson, R. A., and S. P. Perone, "Polarographic, Coulometric, and Stationary Electrode Studies of the Electroreduction of Te(IV) in Alkaline Solution," *J. Electroanal. Chem.*, **23**, 441 (1969).
 Jordan, A. S., "A Theory of Regular Associated Solutions Applied to the Liquidus Curves of the Zn-Te and Cd-Te Systems," *Metal. Trans.*, **1**, 239 (1970).
 Levich, V. G., *Physicochemical Hydrodynamics*, Prentice-Hall, Inc., Englewood Cliffs, New Jersey (1962).
 Lingane, J. J., and L. W. Niedrach, "Potentiometric Titration of +4 and +6 Selenium and Tellurium with Chromous Ion," *J. Am. Chem. Soc.*, **70**, 1997 (1948).
 ———, "Polarography of Selenium and Tellurium. II. The +4 States," *ibid.*, **71**, 196 (1949).
 Loferski, J. J., "Theoretical Considerations Governing the Choice of the Optimum Semiconductor for Photovoltaic Solar Energy Conversion," *J. Appl. Phys.*, **27**, 777 (1956).
 Lyman, T., ed., *Metals Handbook*, rev. ed., Am. Soc. for Metals, Cleveland, OH (1948).
 Lyons, L. E., et al., "Cathodically Electrodeposited Films of Cadmium Telluride," *J. Electroanal. Chem.*, **168**, 101 (1984).
 Menon, M., and U. Landau, "Thickness and Composition Variations along Electrodes in Alloy Plating—A Numerical Model," and "Current Distribution Modeling in Cells with Forced Convection Including Unsteady-state Effects," *Electrochem. Soc. Meet.*, Abstracts 217, 224, Las Vegas (Oct., 1985).
 Mott, N. F., and H. Jones, *The Theory of the Properties of Metals and Alloys*, Dover, New York (1958).
 Newman, J., "Current Distribution on a Rotating Disk below the Limiting Current," *J. Electrochem. Soc.*, **113**, 1235 (1966).
 ———, *Electrochemical Systems*, Prentice-Hall, Englewood Cliffs, NJ (1973).
 Nisancioglu, K., and J. Newman, "Transient Convective Diffusion to a Disk Electrode," *J. Electroanal. Chem.*, **50**, 23 (1974).
 Panicker, M. P. R., et al., "Cathodic Deposition of CdTe from Aqueous Electrolytes," *J. Electrochem. Soc.*, **125**, 566 (1978).
 Pesco, A. M., and H. Y. Cheh, "Current Distribution during the Deposition of Tin-Lead Alloys," *Electrochem. Soc. Meet.*, Abstract 218, Las Vegas (Oct., 1985).
 Puipe, J. Cl., and N. Ibl, "The Morphology of Pulse-Plated Deposits," *Plating*, **67**, 68 (1980).
 Schlichting, H., *Boundary-Layer Theory*, 7th ed., McGraw-Hill, New York (1979).
 Schuhmann, R., "The Free Energy and Heat Content of Tellurium Dioxide and of Amorphous and Metallic Tellurium. The Reduction Potential of Tellurium," *J. Am. Chem. Soc.*, **47**, 356 (1925).
 Seitz, F., *The Physics of Metals*, McGraw-Hill, New York (1943).
 Shinagawa, M., et al., "Studies on the Prewave of Tellurium and Its Photoeffect," *J. Electroanal. Chem.*, **75**, 809 (1977).
 Skyllas-Kazacos, M., "Electrodeposition of CdSe and CdSe + CdTe Thin Films from Cyanide Solutions," *J. Electroanal. Chem.*, **148**, 233 (1983).
 Swathirajan, S., "Potentiodynamic and Galvanostatic Stripping Meth-

- ods for Characterization of Alloy Electrodeposition Process and Product," *J. Electrochem. Soc.*, **133**, 671 (1986).
- Takahashi, M., et al., "Composition and Electronic Properties of Electrochemically Deposited CdTe Films," *J. Appl. Phys.*, **55**, 3879 (1984).
- Tibbals, C. A., "A Study in Tellurides," *J. Am. Chem. Soc.*, **31**, 902 (1909).
- Uosaki, K., et al., "The Photoelectrochemical Behavior of Electrochemically Deposited CdTe Films," *Electrochim. Acta*, **29**, 279 (1984).
- Verbrugge, M. W., "The Periodic Electrodeposition of Alloys," Ph.D. Thesis, Univ. of California, Berkeley (1985).
- Verbrugge, M. W., and C. W. Tobias, "Triangular Current-Sweep Chronopotentiometry at Rotating Disk and Stationary, Planar Electrodes," *J. Electroanal. Chem.*, **196**, 243 (1985a).
- , "A Mathematical Model for the Periodic Electrodeposition of Multicomponent Alloys," *J. Electrochem. Soc.*, **132**, 1298 (1985b).
- White, R., "Potential-Selective Deposition of Copper from Chloride Solutions Containing Iron," *J. Electrochem. Soc.*, **124**, 669 (1977).
- Zanio, K., *Cadmium Telluride*, Semiconductors and Semimetals, **13**, Academic Press, New York (1978).

Manuscript received Feb. 2, 1986, and revision received Sept. 3, 1986.